



COB-2019-1208

STUDY OF ABLATION ON SURFACES OF ZIRCALOY Z-4 IRRADIATED WITH FEMTOSECOND LASER

Paulo Guanabara Júnior

Centro Tecnológico da Marinha em São Paulo – Estrada Iperó-Sorocaba, km 12,5, CEP 18560-000, Iperó-SP
paulo.guanabara@marinha.mil.br;

Alessandro Francelino Nogueira

Centro Tecnológico da Marinha em São Paulo – Estrada Iperó-Sorocaba, km 12,5, CEP 18560-000, Iperó-SP
alessandro.nogueira@marinha.mil.br

Ricardo Elgul Samad

Instituto de Pesquisas Energéticas e Nucleares (IPEN) – Av. Prof. Lineu Prestes, 2242, CEP 05508-000, São Paulo-SP
resamad@ipen.br

Wagner de Rossi

Instituto de Pesquisas Energéticas e Nucleares (IPEN) – Av. Prof. Lineu Prestes, 2242, CEP 05508-000, São Paulo-SP
wderossi@ipen.br

Abstract. *The use of ultrashort femtosecond laser pulses is an alternative for micro-machining on metal surfaces, with several industrial applications, in such areas as aeronautics, aerospace, naval, nuclear, among others, where there is growing concern about service reliability. Thus, markings for traceability purposes should ensure the integrity of the metal as well as allow reading of the marked characters, whether automated or not. In this work, micro-machining of zircaloy Z-4 surfaces using femtosecond laser was performed aiming at the knowledge of the ablation threshold and Scanning Electron Microscopy (SEM) analysis in different images. Obtained from micro-machined traces, energy fluence parameters and laser pulse overlap. The amount of ablated material in this femtosecond laser micro-machining is negligible, which contributes to ensuring that there is no microstructural damage. Such a process resulted in different images, which characterize that there are different optical properties because of the parameters change.*

Keywords: *ultrashort, femtosecond, micro-machining, Zircaloy Z-4, ablation.*

1. INTRODUCTION

Micro-machining, which previously had only been researched in the scientific area, currently has applications in several industrial segments, such as aerospace and aeronautics, medical equipment, microelectronics and automotive, as well as micromotors, microfluidic circuits and microsystems (Samad et al., 2012).

An important factor influencing precision in laser micro-machining is the thermally affected zone (TAZ), extending beyond the laser pulse interaction region, responsible for a phase transformation, altering the material properties. The thermodynamic side effect is intrinsic to the ablation process when pulses longer than approximately 1 picosecond are used, this being the common lasers case, which have a time width of tens of nanoseconds. However, this factor can be minimized by the rapid deposition of energy through ultrashort pulses, ablating the material before the diffusion of heat (Jandeleit et al., 1998 and Pronko et al., 1995). The interaction process of laser irradiation with matter from femtoseconds to nanoseconds, involves many phenomena that occur at different time scales (Bulgakova et al., 2004).

Ultrashort laser pulses of femtoseconds allow a deterministic interaction with a well-defined ablation threshold, but it not only depends on the characteristics of the laser pulse and the type of ablated material. The pulse absorption also depends on the presence of defects in the crystalline structure of these materials. Pre-irradiation by a laser pulse in a material, even below the damage threshold, can create defects in the crystal lattice. This process is called the incubation

effect and is responsible for lowering the damage threshold in pre-irradiated material. Thus, laser pulses that reach the pre-irradiated material have greater ease in the ablation sequence of the material (Ashkenasi et al., 2002).

The surface micro-machining process requires the overlapping of pulses so that the required amount of material is removed. Thus, the ablation threshold and the incubation parameter are important parameters for micro-machining and must be previously known. In this context, this work had its focus in the accomplishment of experiments imposing changes in the variables fluency, repetition rate and incubation parameters by the overlap of pulses.

To obtain the minimum heat transfer condition to the material, suitable process parameters need to be used. Thus, the fluency should be above its ablation threshold. Therefore, the beginning of the work focused on obtaining the low and high fluency regimes, and then micro-machining with process parameters appropriate to the material. For the measurement of the ablation threshold and the incubation parameter, the experimental technique Diagonal Scan (D-Scan) was used, and this technique was introduced by the Lasers and Applications Center of Nuclear and Energy Research Institute (CLA-IPEN), presented in Samad and Vieira Jr. (2006).

Nano and microstructures have been used to alter the physical and chemical properties of metals and ceramic surfaces in order to improve their biocompatibility for medical implants (Schlie et al., 2011). In this regard, Vorobyev and Guo (2007) produced several types of sub-micrometric structures on pure titanium surfaces by femtosecond laser irradiation. Through the use of low and high energy densities of the laser shot, and varying the number of overlapping pulses, several structures were produced such as LIPSS (Laser Induced Periodic Surface Structures), nanostructured LIPSS, nano protrusions as sphere and columnar microstructures whose size varied from a few tens of nanometers to hundreds of micrometers.

As the presence of micro and nano structures on metal surfaces also changes their interaction with light. Some research has been done to control the reflectivity of the surface and hence the perception of its color (Vorobyev and Guo, 2008, Ahsan et al., 2011). The control of shape, size and spacing of machined grids on surfaces is a well-known way to control the reflectivity of light; therefore, ripples formed by nanostructured LIPSS obtained by femtosecond laser irradiation may be a natural approach to accomplish such a task. These characteristics can be controlled by manipulation of some process parameters such as fluency, polarization direction, angle of incidence and scanning speed. The final form comprises self-produced micro and nano grids held in a substantially unidirectional field, covering a large area. In addition to using LIPSS, metal staining has also been produced directly by machining small grooves and microhard arrays on their surfaces. Therefore, the structuring of the surface of the metal in scales from nanometers to hundreds of micrometers allows the control of the optical properties, from UV light to terahertz (Samad et al., 2012).

The purpose of this work is to obtain highly light-absorbing regions on a zircaloy Z-4 alloy surface. This will allow to record serial numbers and bar-codes for tracking sensible parts used in nuclear reactors. For this, several traces were produced with threshold fluency close to those of the corresponding N threshold. Only under these conditions is it possible to produce periodic structures of LIPSS. Since these LIPSS are produced, some extra pulses on these structures break their periodicity creating a network of peaks and valleys that absorb the incident light very efficiently.

2. EXPERIMENTAL DETAILS

The ultrashort pulse has a much shorter time duration than the electron-phonon interaction time, and for this reason, a large amount of material can be removed before most of the energy from the light pulse is transferred to the crystal lattice and heat the material (Samad and Vieira Jr., 2006). The use of lasers to create microstructures on metal surfaces, hitherto widely used in the industrial field is based on Q-switched Nd:YAG (Neodymium-doped yttrium aluminum garnet) lasers with time pulses of some tens of nanoseconds. In this case, however, the heat produced by interaction with the pulses causes melting on the surface and a great deformation on very thin sheet surfaces.

Thus, the femtosecond laser, available in the laboratories of the CLA-IPEN, is an important and considerable alternative to obtain such ablated surfaces without the production of collateral heat. So carrying out the experiments using a Ti sapphire femtosecond laser (Femtopower Compact Pro CE-Phase HP / HR from the manufacturer Femtolasers): amplified by the frequency scanning amplification method that continuously generates pulses of 25 fs (FWHM) centered at 775 nm with 40 nm bandwidth (FWHM), maximum 4 kHz repetition rate and 750 μJ maximum energies per pulse. The drive system for the execution of the machining consists of a table with coordinated X and Y axes movement via Computer Numerical Control (CNC) command, while the Z movement is manual through a micrometer. For all axes the movements have micrometric precision.

Considering the propagation model of a Gaussian beam, for fluency estimation, and the calculation theoretical value of the beam diameter on the sample surface. Thus, the theoretical beam diameter in the sample was determined according to Eq. (1) (Siegman, 1986).

$$\Phi = \frac{4. M^2. \lambda. f}{\pi. \Phi_0} \quad (1)$$

Where: ϕ is the beam diameter at the focus; M^2 is the beam quality factor; λ is the laser wavelength; f is the focal length of the lens and ϕ_0 is the beam diameter at the lens input.

Once the theoretical beam diameter is determined at the sample surface, the energy density per pulse (fluency F_0) is calculated by the ratio of beam energy E to beam area A_f at the focus, as shown in Eq. (2).

$$F_0 = \frac{E}{A_f} \quad (2)$$

The overlap of pulses (N) is calculated from Eq. (3), where f_{rt} is the laser beam repetition rate, Φ is the beam diameter at the focus and v is the beam speed with respect to the sample.

$$N = \frac{f_{rt} \cdot \Phi}{v} \quad (3)$$

We used the D-Scan technique a simple alternative method to measure ultrashort pulse ablation threshold, consisting of traversing a sample longitudinally and transversely in the z and y directions, as shown in Fig. 1 (a), through the waist of the beam, from a position before the waist. Thus, as shown in Fig. 1 (b), a symmetrical profile with two lobes is etched onto the sample surface.

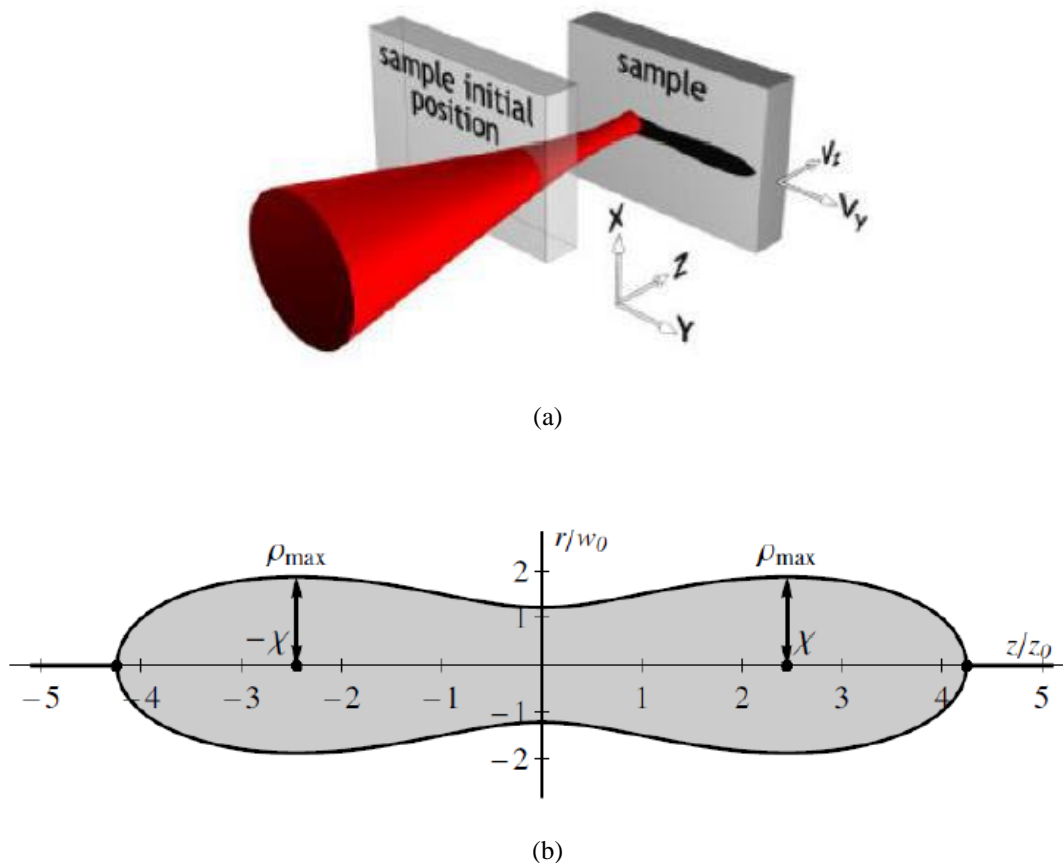


Figure 1. (a) D-Scan technique scheme; (b) profile engraved on the surface of the sample by diagonal movement in position across the waist of the beam.

Adapted from: Samad and Vieira Jr. (2006)

As shown in Samad and Vieira Jr., 2006, The ablation threshold F_{th} for the sample can be measured directly from the geometry of each D-Scan trace Eq. (4) and is determined by:

$$F_{th} = \frac{1}{e \cdot \pi} \frac{E}{\rho_{max}^2} \cong 0.117 \frac{E}{\rho_{max}^2} \quad (4)$$

where E is the pulse energy and ρ_{max}^2 is the half maximum of the cross-section dimension of the engraved profile. If different combinations of repetition rate and speed of beam are used to produce different traces, we may produce several traces with different N overlap values. Consequently, it is possible to obtain F_{th} as a function of the number N of overlapping pulses. Hence, the determination of the ablation threshold comes down to knowledge of the pulse energy and measuring the maximum cross-section dimension of the profile (typically a few tens of microns), which can be done with such Eq. (4) and an optical microscope (Samad and Vieira Jr., 2006).

The SEM (Scanning Electron Microscopy) were used to investigate the sample surface image due to trace micromachining with laser beam parameters. Such as Fluency F_0 [J/cm^2]; Overlapping Pulses N and microscope parameters as Accelerating Voltage, Working Distance and Magnification. Operating with the following microscope parameters: - at 15 kV accelerating voltage; working distance 6.5 mm and 7,000X magnification.

3. RESULTS AND DISCUSSION

The D-Scan method was performed on a sample of Zircaloy Z-4 with dimensions of 10 mm x 10 mm and thickness of 2.0 mm. In the method, 30 traces were performed, with repetition rates of 100 Hz, 500 Hz and 4,000 Hz, energies ranging from $82.25 \pm 2.52 \mu J$ to $88.58 \pm 2.07 \mu J$. With this combination of parameters it was possible to obtain pulse overlap from 0.4 to 17490 pulses in these 30 scratches. The inert gas argon (Ar) with a purity greater than 99.999% with a flow rate of 8.0 L/min was used to protect the atmosphere of the ablated regions. The parameters and results are presented in Fig. 2.

Repetition rate f_{rr}									
4kHz									
Energy E									
$88.58 \mu J \pm 2.07 \mu J$									
Velocity v (mm/s)									
Profile 01	Profile 02	Profile 03	Profile 04	Profile 05	Profile 06	Profile 07	Profile 08	Profile 09	Profile 10
0.05	0.1	0.2	0.5	1.0	2.0	5.0	10.0	20.0	30.0
Overlapping pulses N									
Profile 01	Profile 02	Profile 03	Profile 04	Profile 05	Profile 06	Profile 07	Profile 08	Profile 09	Profile 10
17490	8277	4060	1593	765	367	145	64	30	19.3
Repetition rate f_{rr}									
500 Hz									
Energy E									
$86.46 \mu J \pm 2.03 \mu J$									
Velocity v (mm/s)									
Profile 11	Profile 12	Profile 13	Profile 14	Profile 15	Profile 16	Profile 17	Profile 18	Profile 19	Profile 20
0.05	0.1	0.2	0.5	1.0	2.0	5.0	10.0	20.0	30.0
Overlapping pulses N									
Profile 11	Profile 12	Profile 13	Profile 14	Profile 15	Profile 16	Profile 17	Profile 18	Profile 19	Profile 20
1952	937	449	158	74	36	14.1	6.8	3.2	2.0
Repetition rate f_{rr}									
100 Hz									
Energy E									
$82.25 \mu J \pm 2.52 \mu J$									
Velocity v (mm/s)									
Profile 21	Profile 22	Profile 23	Profile 24	Profile 25	Profile 26	Profile 27	Profile 28	Profile 29	Profile 30
0.05	0.1	0.2	0.5	1.0	2.0	5.0	10.0	20.0	30.0
Overlapping pulses N									
Profile 21	Profile 22	Profile 23	Profile 24	Profile 25	Profile 26	Profile 27	Profile 28	Profile 29	Profile 30
383	180	87	32	14.4	6.7	2.6	1.2	0.6	0.4

Figure 2. Frame with parameters and results in the realization of the experiment D-Scan for Zircaloy Z-4.
 Source: Author

Ten of these micro-machined profile traces, by D-Scan method with 4,000 Hz repetition rate, using the above described combination of parameters, performed on the zircaloy Z-4 sample surface are shown in Figure 3.

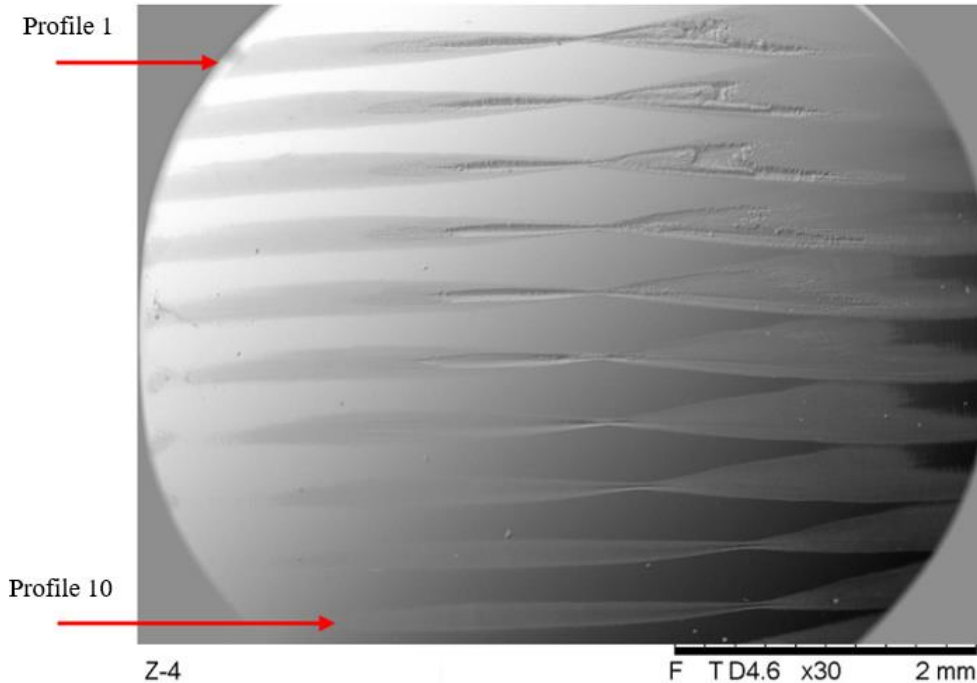


Figure 3. SEM image of the micro-machined profiles 1 to 10 in the Z-4 sample by the D-Scan method with 4,000 Hz repetition rate. Microscope parameters: Accelerating Voltage 15 kV, Working Distance 6.5 mm, 30x magnification.
 Source: Author

Figure 4 shows the points related to the overlap of each of the 30 profiles, where it was possible to trace the function defined by the equation shown in the graph. Thus, any on the laser system that is located above the line will be in the high fluence region for the Zircaloy Z-4. The maximum width ρ^2_{max} of each profile was measured and the corresponding threshold fluency F_{th} (N) was calculated using Eq. 4.

The plot of the ablation threshold F_{th} as a function of the overlap of pulses N, calculated using Eq.3, is shown in graph Fig. 4.

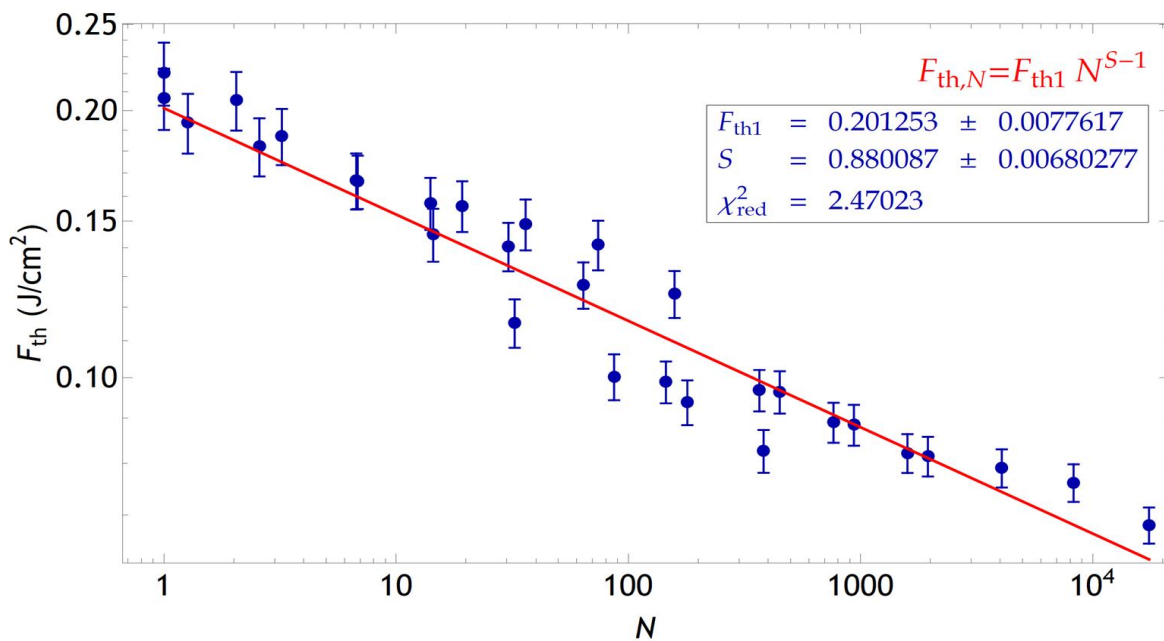


Figure 4. Plot of $F_{th} \times N$, with the adjustment performed by a straight line, using the D-Scan method to determine the ablation threshold for Z-4.
 Source: Author

Analyzing the graphic, it is shown that for Zircaloy Z-4 the ablation threshold is $F_{th} = 0.201 \pm 0.008 \text{ J/cm}^2$ for just one shot and falls linearly with the overlapping pulses N number accumulation, reaching less than half to $N = 1,000$ pulses. Thus, it is necessary to consider this fall in ablation threshold (F_{th}) when performing a continuous machining. As N depends on the ratio of pulse repetition rate to beam displacement speed, it is possible to calculate the fluency for the actual process conditions and thereby verify whether the used fluency is well above the threshold. In this case, unwanted thermal effects may occur.

Micro-machining was then performed on Zircaloy Z-4 sample with different parameters using femtosecond laser to produce such LIPSS. Plot of Figure 4 was used to choose these parameters. The aim was to produce a variety of visible colors on the metal surface to identify periodical structures and then obtain a black surface. Since LIPSS are generated by controlling the fluency, the incident angle, and the polarization of the laser beam, which is a versatile way in modify optical properties, the period of the LIPSS can be controlled, and minimize collateral damage on material and unwanted thermal effects.

The experiments were performed to obtain LIPSS, initially using 2,000Hz repetition rate, $T_p = 30 \text{ fs}$, $f = 20 \text{ mm}$ lens with three different energies $E = 0.2 \mu\text{J}$, $E = 0.4 \mu\text{J}$ and $E = 0.6 \mu\text{J}$. Each one with eight traces with beam speed ranging from $v = 0.25$ to $v = 10$, which results not produced a desired variety of colors. So, a new set of experiments was performed with $f_r = 10,000 \text{ Hz}$ repetition rate, $T_p = 30 \text{ fs}$, $f = 50 \text{ mm}$ lens, and seven different energies. Initially with $E = 1.2 \mu\text{J}$, $E = 2.4 \mu\text{J}$ and $E = 3.6 \mu\text{J}$. Each one with seven traces with beam speed ranging from $v = 2 \text{ mm/s}$ to $v = 25 \text{ mm/s}$. After partial results were noticed on $E = 3.6 \mu\text{J}$ condition, traces without LIPSS. Then adding two more energies $E = 3.0 \mu\text{J}$ and $E = 1.2 \mu\text{J}$.

Were examined the SEM images due to trace with femtosecond laser beam micromachining, generated using the above conditions and laser beam parameters, whose microscope parameters indicated in the following images as accelerating voltage, working distance and magnification were kept. Such images shown with the same beam speed $v = 2 \text{ mm/s}$ and overlapping pulses $N = 4.4 \text{ kHz}$, with higher energy E and fluency F beginning a process of degeneration of LIPSS formation. Considering The SEM image, in Fig. 5, due to trace micromachining with laser beam, having fluency $F = 0.71 \text{ J/cm}^2$, beam speed $v = 2 \text{ mm/s}$ and energy $E = 1.2 \mu\text{J}$ was generated with laser induced periodic surface structures (LIPSS), with small grooves and microhard arrays shown on their surfaces.

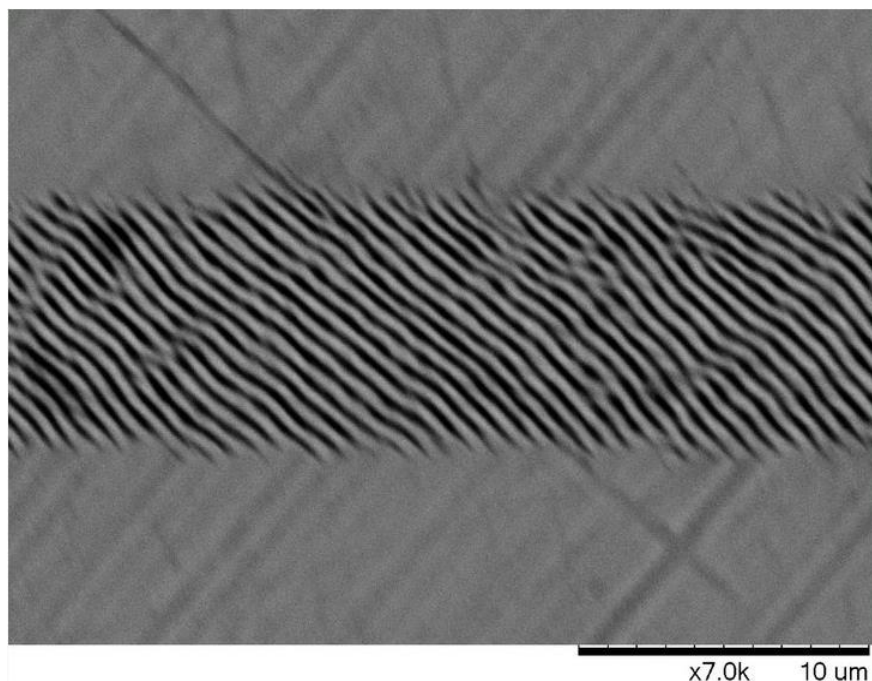


Figure 5. SEM image in Zircaloy Z-4 sample. Laser beam parameters: Fluency $F_0 = 0.71 \text{ J/cm}^2$, overlapping pulses $N = 4.4$. Microscope parameters: Accelerating Voltage 15 kV, Working Distance 6.5 mm, 7000x magnification.
Source: Author

The SEM image below, a scratch produced with high energy $E = 2.4 \mu\text{J}$ and fluency $F = 1.42 \text{ J/cm}^2$ with the same beam speed $v = 2 \text{ mm/s}$ and $N = 4.4$, keeping LIPSS formation, but beginning a process of its degeneration, as shown in Fig.6.

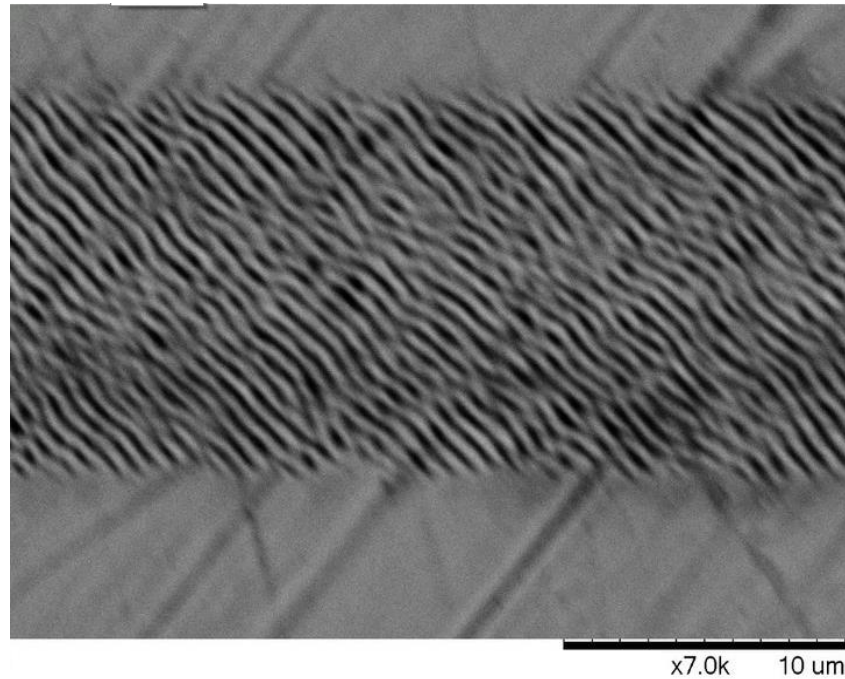


Figure 6. SEM image of Zircaloy Z-4 sample. Laser beam parameters: Fluency $F_0 = 1.42 \text{ J/cm}^2$, overlapping pulses $N = 4.4$. Microscope parameters: Accelerating Voltage 15 kV, Working Distance 6.5 mm, 7000x magnification.
Source: Author

The SEM image in Fig. 7 shows a scratch produced with higher energy and fluency, respectively $E = 3.0 \text{ } \mu\text{J}$, $F = 1.78 \text{ J/cm}^2$ with the same beam speed $v = 2 \text{ mm/s}$ and $N = 4.4$. Under these conditions there is clearly a severe destruction of the LIPSS.

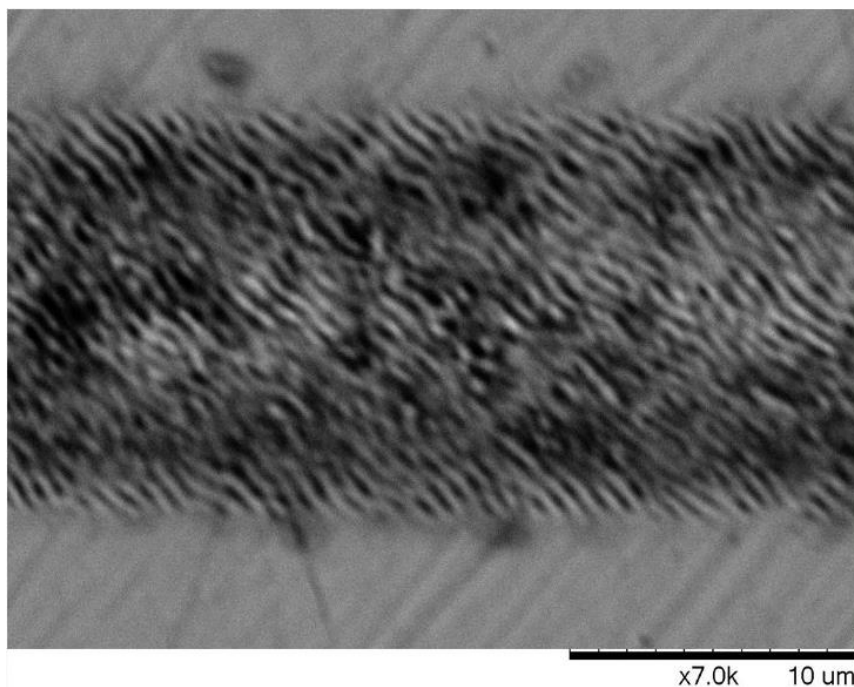


Figure 7. SEM image due to trace micro-machining in Zircaloy Z-4 sample. Laser beam parameters: Fluency $F_0 = 1.78 \text{ J/cm}^2$, overlapping pulses $N = 4.4$. Microscope parameters: Accelerating Voltage 15 kV, Working Distance 6.5 mm, 7000x magnification.
Source: Author

4. CONCLUSION AND FUTURE WORKS

Threshold fluence for Zircaloy Z-4 decreases dramatically with increasing N pulse overlap as shown by the D-Scan technique. LIPSS production is only possible when the fluence used is not much higher than that of threshold. Thus, the relationship between laser beam travel speed and pulse repetition rate needs to be controlled to determine N overlap and choose a suitable fluence for this condition. With this procedure it was possible to obtain traces with periodic structures of the LIPSS type. Note that the same beam speed $v = 2$ mm/s and overlapping pulses $N = 4.4$, a fluence of 0.7 J/cm² with pulses $N = 4.4$ produced very well defined LIPSS. Increasing this fluence to 1.78 J.cm² begins to destroy the structure's periodicity and increase light absorption. A path for future works to produce extra pulses on these structures break their periodicity creating a network of peaks and valleys that absorb the incident light more efficiently.

5. ACKNOWLEDGEMENTS

The authors thank FAPESP (grant 2013/26113-6), IPEN, Technological Center of the Navy in São Paulo (CTMSP) and Aramar Industrial Nuclear Center (CINA) for the support given to the development of this research.

6. REFERENCES

- Ahsan, M. S., Ahmed, F.; Kim, Y. G., Lee, M. S., Jun, M. B. G., 2011. "Colorizing stainless steel surface by femtosecond laser induced micro/nano-structures". *Applied Surface Science*. Vol. 257, No. 17, pp. 7771-7777.
- Ashkenasi D., Rosenfeld A., Stoian R., 2002. "Laser-induced incubation in transparent materials and possible consequences for surface and bulk micro-structuring with ultrashort pulses". In *Commercial and Biomedical Applications of Ultrafast and Free-Electron Lasers - Society of Photo-Optical Instrumentation Engineers (SPIE)*. Vol. 4633.
- Bulgakova N.M., Stoian R., Rosenfeld A., Hertel I.V., Campbell E.E.B., 2004. "Electronic transport and consequences for material removal in ultrafast pulsed laser ablation of materials". *Physical Review B - Condensed Matter and Materials Physics*. Vol. 69, No. 5, 054102.
- Jandeleit J., Horn A., Weichenhain R., Kreutz E.W., Poprawe R., 1998. "Fundamental investigations of micromachining by nano- and picosecond laser radiation". *Applied Surface Science*. Vol. 127, No. 1, pp. 885-891.
- Pronko P.P., Dutta S.K., Squier J., Rudd J.V., Du D, Mourou G., 1995. "Machining of sub-micron holes using a femtosecond laser at 800 nm". *Optics Communications*. Vol. 114, No. 1, pp.106-110.
- Samad R.E., Machado L.M., Vieira Jr., N.D., De Rossi W., 2012. "Ultrashort Laser Pulses Machining", In *Laser Pulses - Theory, Technology, and Applications, InTechOpen, I. Peshko (Ed.)*. pp.143-174.
- Samad R.E. and Vieira Jr. N.D., 2006. "Geometrical method for determining the surface damage threshold for femtosecond laser pulses". *Laser Physics*. Vol. 16, No. 2, pp. 336-339.
- Schlie, S., Fadeeva, E., Koroleva, A., Ovsianikov, A., Koch, J., Ngezahayo, A., Chichkov, B. N., 2011. "Laser-based nanoengineering of surface topographies for biomedical applications". *Photonics and Nanostructures – Fundamentals and Applications*. Vol. 9, No. 2, pp. 159-162.
- Siegman A.E., 1986. *Lasers*. University Science Books, Salsalito, CA, United States, 1th edition.
- Vorobyev, A. Y. and Guo, C., 2007. "Femtosecond laser structuring of titanium implants". *Applied Surface Science*. Vol. 253, No. 17, pp. 7272-7280.
- Vorobyev, A. Y. and Guo, C., 2008. "Colorizing metals with femtosecond laser pulses". *Applied Physics Letters*. Vol. 92, No. 4, 041914.

7. RESPONSIBILITY NOTICE

The authors are the only responsible for the printed material included in this paper.